

## **Symplectic calculation of the homoclinic tangles of the ideal separatrix of the simple map**

Alkesh Punjabi<sup>1</sup> and Halima Ali<sup>1</sup>

<sup>1</sup>*Hampton University, Hampton, VA, 23668, USA*

ABSTRACT: The simplest symplectic map that has the generic topology of the divertor tokamaks is the simple map [1]. The generating function for the simple map and the symplectic map equations can be transformed to natural canonical coordinates  $(\psi, \theta, \varphi)$  [2] through a canonical transformation.  $\psi$  is toroidal flux,  $\theta$  is poloidal angle, and  $\varphi$  is toroidal angle. The natural canonical coordinates are invertible to real physical space [3]. The simple map in natural canonical coordinates is then integrated to calculate the symplectic homoclinic tangles of the ideal separatrix under the influence of qualitatively different kinds of magnetic perturbations, and the tangles are inverted to the real physical space. Ideal separatrix is a degenerate manifold and is the most sensitive to asymmetries. Symplectic homoclinic tangles of the ideal separatrix from different kinds of perturbations, phase differences, and amplitudes are calculated. For some perturbations, the tangles have very pronounced lobes. Implication of these results for physics of edge plasmas is discussed. This work is supported by the US DOE grants DE-FG02-01ER54624 and DE-FG02-04ER54793. This research used resources of the NERSC, supported by the Office of Science, US DOE, under contract DE-AC02-05CH11231.

The simple map [1] is the simplest symplectic map that has the magnetic topology of divertor tokamaks. The simple map is a very valuable construct to study the generic topological effects of magnetic perturbations on the trajectories of magnetic field lines in divertor tokamaks. The simple map preserves the topological invariance of the Hamiltonian system. The equilibrium generating function of the simple map in canonical representations have the simplest mathematical expressions. There are three canonical representations for the simple map: the physical, natural, and the action-angle [2]. Of these three canonical representations, the natural coordinates are the most useful [2] because the natural coordinates are invertible to real physical space [3] and it is easy to add doubly periodic sinusoidal magnetic perturbations. Field line trajectories can be integrated across the separatrix surface which cannot be done in magnetic coordinates. In this paper, we calculate the symplectic homoclinic tangles of the ideal separatrix manifold of the simple map from qualitatively

different kinds of magnetic perturbations and give the effects of these tangles on the tokamak plasmas.

In the natural canonical coordinates the magnetic field is  $\mathbf{B}=\nabla\psi\times\nabla\theta+\nabla\phi\times\nabla\chi(\psi,\theta,\phi)$ .  $\theta$  is the poloidal angle, and it is the canonical position;  $\psi$  is the toroidal magnetic flux inside the magnetic surface, and it is the canonical momentum;  $\phi$  is the toroidal angle, and it plays the role of canonical time;  $\chi$  is the poloidal flux, and it plays the role of the Hamiltonian for the trajectories of field lines. The equilibrium generating function is  $\chi_0(\psi,\theta)=\psi-(2\sqrt{2/3})\psi^{3/2}\sin^3(\theta)$ . The natural coordinates are inverted to physical coordinates using the canonical transformation  $x=\sqrt{(2\psi/B_0)}\cos(\theta)$  and  $y=\sqrt{(2\psi/B_0)}\sin(\theta)$  with  $B_0$  an arbitrary magnetic field. We take  $B_0=1$  Tesla. The physical coordinates  $(x,y)$  are connected to cylindrical coordinates  $(R,Z)$  by  $R=R_0+x$ , and  $Z=Z_0+y$ .  $(R_0,Z_0)$  is the location of magnetic axis. The equilibrium surfaces can be calculated analytically.  $\chi=0$  gives the magnetic axis;  $0<\chi<1/6$  gives closed surfaces and the surfaces in the private flux region;  $\chi=1/6$  gives the separatrix surface; and  $\chi>1/6$  gives the open surfaces. The equilibrium magnetic surfaces are shown in Fig. 1. The symplectic map equations are  $\psi_{n+1}=\psi_n-k[\partial\chi(\psi_{n+1},\theta_n,\phi_n)/\partial\theta_n]$ , and  $\theta_{n+1}=\theta_n+k[\partial\chi(\psi_{n+1},\theta_n,\phi_n)/\partial\psi_{n+1}]$ .  $k$  is the map parameter, and it is the step size of symplectic integration. We take  $k=2\pi/360$ . Here  $\chi(\psi,\theta,\phi)=\chi_0(\psi,\theta)+\chi_1(\psi,\theta,\phi)$ .  $\chi_1$  is the magnetic perturbation. The perturbation is expressed as sum of Fourier modes  $\chi_1(\psi,\theta,\phi)=\sum_{(m,n)}\delta_{mn}\cos(m\theta-n\phi+\vartheta_{mn})$ .  $m$  and  $n$  are the poloidal and toroidal mode numbers,  $\vartheta_{mn}$  are the phases, and  $\delta_{mn}$  are the amplitudes. The map equations are for forward advance  $(\psi_n,\theta_n,\phi_n)\rightarrow(\psi_{n+1},\theta_{n+1},\phi_{n+1})$ . In this case, if the radial dependence of the amplitudes is ignored, the first map equation for  $\psi$  reduces to a third degree polynomial in  $\sqrt{\psi_{n+1}}$  and then it is possible to solve it analytically; the second equation in  $\theta_{n+1}$  is explicit and so solved readily. For the backward map  $(\psi_{n+1},\theta_{n+1},\phi_{n+1})\rightarrow(\psi_n,\theta_n,\phi_n)$ , the map equation for  $\theta_n$  is implicit, and the map equation for  $\psi_n$  is explicit. Here we will set  $\delta_{mn}(\psi)=\delta$ , ignoring the radial dependence of Fourier modes.

The X-point ( $\theta=\pi/2,\psi=1/2$ ) is a hyperbolic saddle point, and the unperturbed separatrix surface is a degenerate manifold  $\mathcal{M}$  where the stable and unstable manifolds,  $\mathcal{M}^S$  and  $\mathcal{M}^U$ , coincide. Magnetic perturbation breaks the degeneracy of  $\mathcal{M}$  and splits it into  $\mathcal{M}^S$  and  $\mathcal{M}^U$  as  $\mathcal{M}$  is advanced forward and backward in canonical time under the influence of the

symmetry breaking perturbation, forming the homoclinic tangles in the principal plane of tokamak. Here we calculate homoclinic tangles for two kinds of perturbations: the topological noise and field errors with locked modes  $(3,1) + (4,1) + (6,2) + (7,2) + (8,2) + (9,3) + (10,3) + (11,3) + (12,3)$  with common amplitude  $\delta_{\text{NOISE}} = 2 \times 10^{-5}$ , and the type I ELM represented by the locked peeling-ballooning modes  $(30,10) + (40,10)$  with amplitude  $\delta_{\text{ELM}} = 10^{-4}$ . We calculate the symplectic homoclinic tangles of the ideal separatrix of the simple map. We advance  $2 \times 10^5$  points on this surface a single toroidal circuit forward and backward. The results are shown in Figs. 2 and 3.

The edge plasma in divertor tokamaks plays the critical role in the L to H mode transition [4-8]. Homoclinic tangles cause large distortions of magnetic topology of the tokamak near the X-point. Lobes near the X-point in the MAST tokamak that may be caused by tangles are seen experimentally [9]. To our knowledge, we are the first to symplectically calculate these tangles in physical space. Large distortions of magnetic topology can have important consequences on the plasma confinement. Some of the possibilities are that the radial displacement of mobile passing electrons on tangles can create radial electric fields and currents giving a poloidal  $\mathbf{E} \times \mathbf{B}$  plasma flow [4-8], and the resulting  $\mathbf{j} \times \mathbf{B}$  force may give the spin-up of plasma that may contribute to L to H mode transition [4-8]. Work has application beyond tokamaks since the approach is general and generic for  $1\frac{1}{2}$  degree of Hamiltonian systems, and therefore can be of value to nonlinear dynamics of Hamiltonian systems.

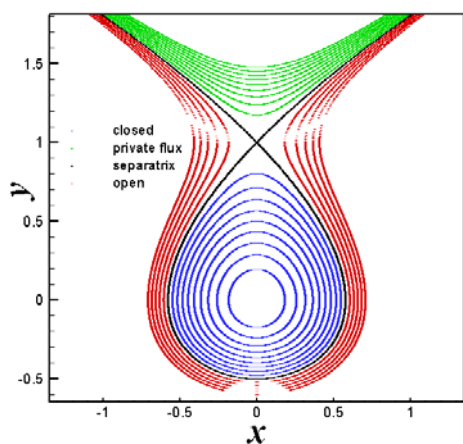


Fig. 1. The equilibrium magnetic geometry of the simple map.

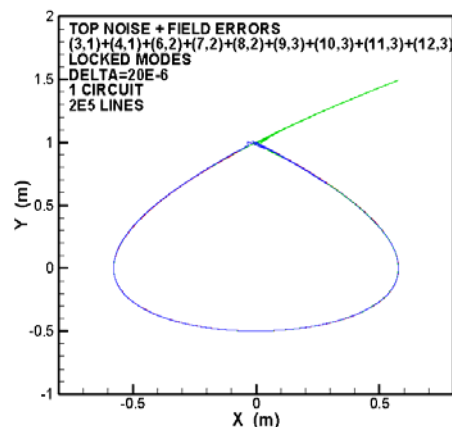


Fig. 2a. Homoclinic tangles of the ideal separatrix of the simple map for the topological noise and field errors.

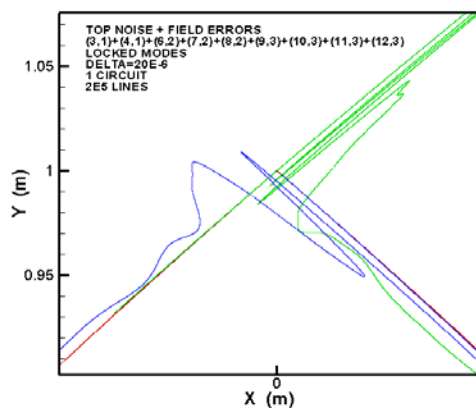


Fig. 2b. An enlarged view of Fig. 2a.

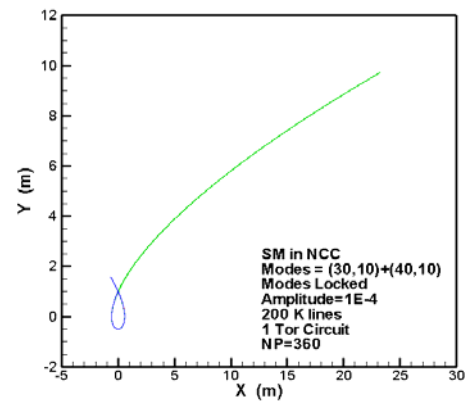


Fig. 3a. Fig. 2a. Homoclinic tangles of the ideal separatrix of the simple map for the peeling-ballooning mode for type I ELM.

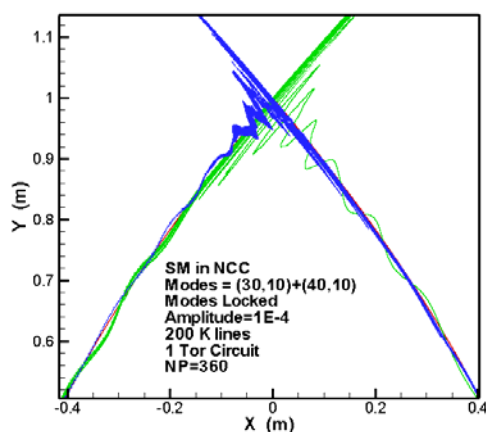


Fig. 3b. An enlarged view of Fig. 3a.

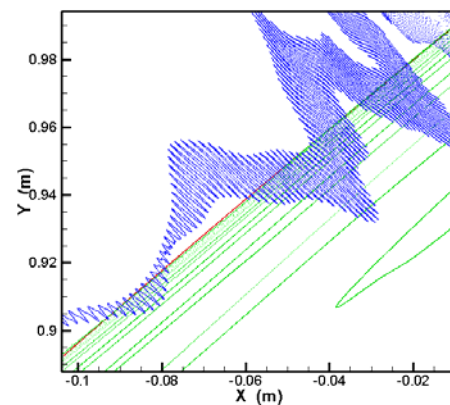


Fig. 3c. An enlarged view of Fig. 3b.

## References

- [1] A. Punjabi, A. Verma, and A. Boozer, *Phys. Rev. Lett.* **69** 3322 (1992)
- [2] A. Punjabi and H. Ali, *Phys. Plasmas* **15** 122502 (2008)
- [3] A. Punjabi, H. Ali, T. Evans, and A. Boozer, *Phys. Lett. A* **364** 140 (2007)
- [4] P.H. Diamond, and Y.-B. Kim, *Phys. Fluids B* **3** 1626 6 (1991)
- [5] S.B. Korsholm et al, *Plasma Phys. Control. Fusion* **43** 1377 (2001)
- [6] R.J. Taylor et al, *Phys. Rev. Lett.* **63** 2365 (1989)
- [7] H. Wobig, and J. Kisslinger, *Plasma Phys. Control. Fusion* **42** 823 (2000)
- [8] A. Boozer, *Rev. Modern Phys.* **6** 1071 (2004)
- [9] A. Kirk et al, *Phys.Rev. Lett.* **108** 255003 (2012)